AIAA JOURNAL
Vol. 49, No. 2, February 2011

Technical Notes

Effect of Inflow Boundary Conditions on the Turbulence Solution in Internal Flows

Upender K. Kaul*
NASA Ames Research Center,
Moffett Field, California 94035

DOI: 10.2514/1.J050532

Nomenclature

D_i	=	diffusivities
Pr_t	=	turbulent Prandtl number
p'	=	fluctuating pressure
U_∞	=	reference velocity
u_i	=	time-averaged flow velocity vector
u'_i	=	fluctuating flow velocity vector
V_i	=	contravariant velocity vector
$\Delta\tau$	=	integration time stepsize
δ_{ij}	=	Kronecker delta
θ	=	time-averaged temperature
θ'	=	fluctuating temperature
μ	=	dynamic laminar viscosity

Subscripts

i, j, k	=	indices for coordinate directions

Superscript

T	=	vector transpose

I. Introduction

A FULLY implicit numerical method for the solution of three-dimensional transport equations of fluid dynamics cast in generalized curvilinear coordinates has been enhanced to demonstrate the effect of inflow conditions on the downstream development of internal flow in a channel. The effect of inlet boundary conditions on turbulence kinetic energy k and the dissipation rate ϵ on the downstream developing flow is assessed in terms of local values of k and Reynolds stress profiles. It is shown that the effect of inflow conditions lasts well over tens of channel heights downstream, before the flow eventually attains a fully developed state. This has an important bearing on turbulent flow (especially internal turbulent flow) simulation results where the characteristic dimensions of interest of engineering systems are much shorter. In some simulations, the solution sought may be in serious error if the inflow conditions chosen are not physically realistic. It is therefore important to account for the effect of wind-tunnel inlet turbulence levels when comparing wind-tunnel experimental data with predictions from a given flow simulation. This study serves as a guide in the prescription of inflow boundary conditions on k and ϵ in simulating laminar to turbulence transition in such flows. Also, the enhanced fully implicit method presented here is demonstrated to improve the convergence to steady state by 2 orders of magnitude for a fully developed turbulent channel flow at Reynolds numbers (based on the channel height) of 7700 and 12,300 with the Chien k-ϵ turbulence model over the previous semi-implicit method developed by the author, where the source terms are treated explicitly. For the case of downstream developing flow, 4 orders of magnitude improvement in convergence to steady state has been realized. The solution of transport equations in fluid dynamics involves solving mixed parabolic-hyperbolic systems. Some of these systems can be very stiff and demanding on the computational resources. Thus, they can require long integration times to achieve a steady state. One such stiff system is a two-equation set of partial differential equations governing turbulence kinetic energy, k, and its dissipation rate, ϵ. These two quantities define the dynamic turbulence viscosity, μ_t, required for a Reynolds Averaged Navier–Stokes (RANS) computation, according to the relation

$$\mu_t = C_\mu f_\mu \rho k^2/\epsilon \tag{1}$$

where $k = \frac{1}{2}\overline{u'_i u'_i}$ and $\epsilon = \frac{\mu}{\rho}\overline{u'_{i,j} u'_{i,j}}$. This relation is based on the Boussinesq approximation

$$-\rho\overline{u'_i u'_j} = \mu_t[\partial_j u_i + \partial_j u_i] - \frac{2}{3}\rho k\delta_{ij} \tag{2}$$

Similarly, for the energy equation, ignoring the pressure-dilatation correlation term, $-\overline{p'\partial_j u'}$, the Boussinesq approximation can be extended to temperature-velocity correlation

$$-\rho\overline{u'_i\theta'_j} = \frac{\mu_t}{Pr_t}\partial_i\theta \tag{3}$$

There is a vast amount of literature available on the subject of turbulence modeling, especially the two-equation models of turbulence. Some of the relevant work on the subject [1–10] is referenced here. However, the focus of the present study is not so much on the art of turbulence modeling, as 1) on the numerical approach to solving the governing equations for turbulence kinetic energy and its dissipation rate and 2) on the effect of inflow turbulence boundary conditions, especially for internal flows.

A well-established ΔQ implicit approximate factorization (AF) algorithm of Beam and Warming [11] and Briley and McDonald [12] is in wide use currently in various CFD methodologies. This AF algorithm was extended to the semi-implicit solution of the three-dimensional equations of turbulence kinetic energy and dissipation rate by the author [5] and through an axisymmetric study [6]. Subsequently, a number of steady-state RANS computational studies have been carried out using the author's approach (e.g., [7–9]).

The fully implicit solution methodology [10] for turbulence kinetic energy and dissipation rate, enhanced through source term linearization and presented here, is based on this AF algorithm and the semi-implicit method of the author [5].

A multicomponent transport in any fluid flow, compressible or incompressible, of various chemical species, temperature (for incompressible flow), salinity or any turbulence property such as the kinetic energy and its dissipation rate is governed by an equation in Cartesian coordinates of the form

$$\partial_t Q + (F_i - F_{v_i})_{,i} = S \tag{4}$$

Presented as Paper 2010-4743 at the 40th AIAA Fluid Dynamics Conference, Chicago, IL, 28 June–1 2010; received 5 March 2010; revision received 22 October 2010; accepted for publication 28 October 2010.

*Fundamental Modeling and Simulations Branch, NASA Advanced Supercomputing (NAS) Division. Associate Fellow AIAA.

where the solution vector is given by

$$Q = [\rho\phi_1, \rho\phi_2, \ldots, \rho\phi_n]^T$$

the "inviscid flux vector" is given by

$$F_i = [\rho u_i\phi_1, \rho u_i\phi_2, \ldots, \rho u_i\phi_n]^T$$

the "viscous flux vector" is given by

$$F_{v_i} = [D_1\partial_i\phi_1, D_2\partial_i\phi_2, \ldots, D_n\partial_i\phi_n]$$

and the source terms are represented as

$$S = S[\rho, \phi_i, {}_{[i=1,2,\ldots,n]}; \ldots)$$

The density ρ is identically equal to 1 for incompressible flow and the ϕ_i are the transport variables.

This set of equations can be solved independently after the five fluid dynamic variables, ρ, ρu_i and the internal energy are updated at the end of each time step for compressible flow; for incompressible flow u_i and the pressure are updated. This decoupling of the transport equations from the basic fluid dynamic conservation equations of mass (continuity equation) and momentum (and additionally, energy in compressible flow) offers a flexibility and ease in obtaining the numerical solution of a given fluid flow problem [5,6].

The normalized governing equations [Eq. (4)] for k and ϵ in generalized curvilinear coordinates are given by the following 2×2 system

$$\partial_\tau\bar{Q} + \partial_{\chi_i}(\bar{F}_i - \bar{F}_{vi}) = \frac{S}{J}$$

where the time and spatial coordinate transformations are given by, respectively

$$\tau \equiv t$$

and

$$\chi_j = \chi_j(x_i, t)$$

where $\chi_j = (\xi, \eta, \zeta)$ and $x_i = (x, y, z)$, and where the solution vector

$$\bar{Q} = \frac{1}{J}[\rho k, \rho\epsilon]^T$$

and the flux vectors are given by

$$\bar{F}_i = \frac{1}{J}[\rho k V_i, \rho\epsilon V_i]^T$$

and

$$\bar{F}_{vi} = \frac{1}{JRe_\infty}[\mu_k\nabla\chi_i.\nabla\chi_i\partial_{\chi i}k, \mu_\epsilon\nabla\chi_i.\nabla\chi_i\partial_{\chi i}\epsilon]^T$$

Assuming a time-invariant grid, the Jacobian and the contravariant velocities are given, respectively, by

$$J = \frac{\partial\chi_i}{\partial x_i}$$

and

$$V_i = u_j\partial_{x_j}\chi_i$$

and ∇ is the gradient operator. The flux vector, $\bar{F}_{vi}$, is redefined as

$$\bar{F}_{vi} = \frac{\alpha}{\rho}[\partial_i(\rho k), \partial_i(\rho\epsilon)]^T - \frac{\alpha}{\rho^2}[\rho k, \rho\epsilon]^T\partial_i\rho$$

where

$$\alpha = \frac{\nabla\chi_i\nabla\chi_i}{JRe_\infty}\begin{bmatrix}\mu_k & 0\\ 0 & \mu_\epsilon\end{bmatrix}$$

where Re_∞ is the reference Reynolds number, and the second term is lumped with the source term, S.

The source terms are given by

$$S = \frac{1}{Re_\infty}\begin{bmatrix} P - \rho\epsilon(1 + M_t^2)Re_\infty - f, \\ C_1\left(\frac{\epsilon}{k}\right)P - C_2 f_2\rho\left(\frac{\epsilon^2}{k}\right)Re_\infty - g \end{bmatrix}^T \tag{5}$$

The compressibility correction term due to Sarkar et al. [13] (as used by [14]) is represented as $\rho\epsilon M_t^2$, where $M_t^2 = 1.5k/a^2$ and $a^2 = \gamma p/\rho$, and the kinetic energy production term due to the mean shear is given by

$$P = -\rho\overline{u_i'u_j'}u_{ij}$$

or by

$$P = \left[\mu_t(u_{i,j} + u_{j,i}) - \frac{2}{3}\rho k Re_\infty\delta_{ij}\right]u_{i,j}$$

The turbulent viscosity, μ_t, is given by

$$\mu_t = C_\mu f_\mu\rho(k^2/\epsilon)Re_\infty$$

where C_μ is a constant, f_μ is a function that accounts for the low Reynolds number dependence of C_μ, and $\mu_k = \mu + \mu_t/\sigma_k$, $\mu_\epsilon = \mu + \mu_t/\sigma_\epsilon$ and $\sigma_k, \sigma_\epsilon$ are the turbulent Prandtl numbers for the k and ϵ transport processes, respectively. The function, f_2, is prescribed [15] as $f_2 = 1 - \frac{0.4}{1.8}\exp(-\rho k^2 Re_\infty/6\mu\epsilon)$.

The relevant constants and the low Reynolds number correction terms, $f = 2\mu\frac{k}{y^2}$ and $g = 2\mu\frac{\epsilon}{y^2}\exp(-c_4 y^+)$, are given in [3], where y is the normal distance from the wall. These source terms [3] are locally linearized in time to demonstrate the efficacy of the fully implicit scheme. However, this linearization can be extended to any other set of source terms, i.e., any particular turbulence model, to demonstrate the power of the implicit scheme presented here. The choice of the turbulence model is immaterial here; the numerical method presented here can be applied with equal promise to any low Reynolds number model. Also, to demonstrate the fully implicit scheme here, it is sufficient to treat incompressible flow. For incompressible flow, the term $\delta_{ij}u_{i,j}$ in the definition of the production term P and the compressibility correction term are identically zero.

II. Numerical Method

The k-ϵ system in generalized coordinates is integrated using the implicit noniterative approximate factorization algorithm of Beam and Warming [11]. The essential details of the scheme are given below.

Writing the finite difference expression for the governing equation in generalized coordinates, we have

$$\frac{Q^{n+1}}{J^{n+1}} + \Delta\tau[\delta_{\chi_i}(\bar{F}_i - \bar{F}_{v_i})^{n+1} - (S/J)^{n+1}] = \frac{Q^n}{J^n}$$

where the time differencing is first-order (Euler) implicit, and the spatial derivatives are approximated by the central-differencing operator δ_{χ_i}.

Linearizing the flux vectors and the source terms locally in time, this equation can be written as

$$\{(I - \Delta\tau J^{n+1}\bar{T}^n) + J^{n+1}\Delta\tau[\delta_{\chi_i}(\bar{M}_i^n - \bar{M}_{vi}^n)]\}(Q^{n+1} - Q^n)$$
$$= \left(\frac{J^{n+1}}{J^n} - I\right)Q^n + \Delta\tau\frac{J^{n+1}}{J^n}S^n - \Delta\tau J^{n+1}\delta_{\chi_i}[\bar{F}_i - \bar{F}_{vi}]$$

where the Jacobian matrix of the flux vector $\bar{F}_i$ is given by

$$\bar{M}_i = (\bar{A}, \bar{B}, \bar{C}) = \partial_{\bar{Q}}\bar{F}_i^n = \frac{1}{J^n}\begin{bmatrix} V_i 0 \\ 0 V_i \end{bmatrix}$$

For time-invariant grids, the ΔQ form of this governing equation reduces to

$$\{(I - \Delta\tau J\bar{T}^n) + J\Delta\tau[\delta_{\chi_i}(\bar{M}_i^n - \bar{M}_{vi}^n)]\}(Q^{n+1} - Q^n) = \Delta\tau S^n - \Delta\tau J\delta_{\chi_i}[\bar{F}_i - \bar{F}_{vi}]$$

The Jacobian matrices, $M_{vi} = \partial\bar{F}_{vi}/\partial\bar{Q}$ and $\bar{T} = \partial\bar{S}/\partial\bar{Q}$ of the viscous flux vector and the source term, respectively, are obtained similarly. The right-hand side (RHS) of this equation is calculated explicitly, assuming a time-invariant grid, and the left hand side is factored approximately. Then, we have

$$[I + \Delta\tau JN^{-1}\delta_\xi(\bar{A}^n - \bar{A}_v^n) + \epsilon_i\nabla_\xi\Delta_\xi][I + \Delta\tau JN^{-1}\delta_\eta(\bar{B}^n - \bar{B}_v^n) + \epsilon_i\nabla_\eta\Delta_\eta] \times [I + \Delta\tau JN^{-1}\delta_\zeta(\bar{C}^n - \bar{C}_v^n) + \epsilon_i\nabla_\zeta\Delta_\zeta](Q^{n+1} - Q^n) = N^{-1} \times \mathrm{RHS} - \epsilon_e[(\nabla\chi_i\Delta\chi_i)^2]Q^n$$

where $N = [I - \Delta\tau J\bar{T}^n]$, ∇ and Δ are first-order forward- and backward-difference operators, ϵ_i is the implicit second-order smoothing parameter, and ϵ_e is the explicit fourth-order smoothing parameter. The smoothing terms are added to damp the high frequency oscillations in the solution which arise out of the central-difference approximation of the spatial derivatives.

Numerical values for the explicit smoothing parameter ϵ_e and the implicit smoothing parameter ϵ_i were fixed for all the simulations at 1.E-05 and 3.E-05, respectively. For developing flow, same time step was used for the mean flow solver as for the transport equation solver. Using very small smoothing parameters, the turbulence solution obtained is of a high fidelity. No artificial constraints on the turbulence viscosity were imposed that are used in some current turbulence solvers.

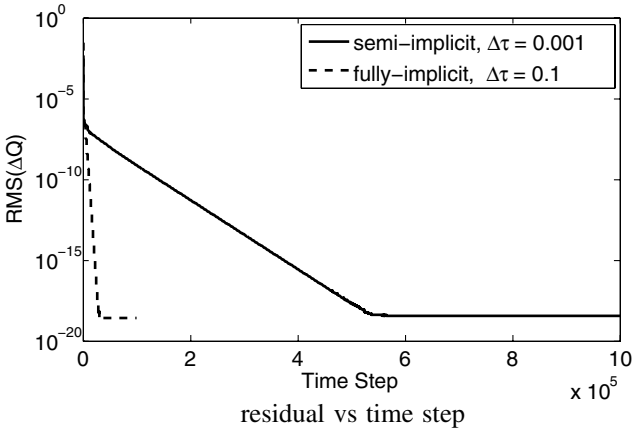

Fig. 1 Convergence history for a fully developed flow at $Re = 7700$: change in the root mean square residual, RMS-DELQ, of the k-ϵ solution vector between two successive time levels.

III. Initial and Boundary Conditions

Two sets of simulations have been carried out to test the fully implicit algorithm. The first set corresponds to the fully developed turbulence in a channel and the second set corresponds to the entrance length problem. Initial conditions and wall boundary conditions are prescribed for the fully developed case. For the developing flow case, initial conditions, inflow, ouflow and wall boundary conditions are prescribed. Inflow profiles for k and ϵ are prescribed as follows.

Assuming a characteristic mixing length scale, $l = 0.14L$, based on correlation-based arguments [16], where the channel semiheight is represented by L; the turbulence kinetic energy and the dissipation rate are given by

$$k = 1.5(U_\infty T_{\mathrm{int}})^2$$

and

$$\epsilon = C_\mu^{3/4}k^{1.5}/l$$

where T_{int} is the turbulence intensity.

In the Chien model, k and ϵ are set to zero at the walls. The homogeneous k and ϵ boundary conditions were imposed implicitly.

Outflow boundary conditions on all the variables are prescribed as $\phi_{xx} = 0$. For the developing flow, uniform inlet pressure and velocity is prescribed and global mass conservation is enforced.

IV. Results

The fully implicit method presented here is compared with the semi-implicit method of the author [5,7] via convergence characteristics of the two techniques. First, the fully developed case is discussed, followed by the downstream developing case.

A. Fully Developed Flow Simulations

Fully developed simulation is essentially a one-dimensional problem. The linear grid in the flow-normal direction contained 99 points, chosen to be fine enough to recover a few points below $y^+ = 1$.

The present predictions are compared with the experiment of Kreplin and Eckelmann [17] and the direct numerical simulation of Kim et al. [18]. A fully developed turbulent channel flow at a Reynolds number of 7700 based on the channel height was calculated and then compared with these data.

An improvement in convergence rate for the fully implicit method is shown in Fig. 1, corresponding to a turbulent intensity, $T_{\mathrm{int}} = 0.1$. The largest time step, $\Delta\tau$, that ensures a stable solution with the semi-implicit approach [5,7] was 0.001, whereas with the present fully implicit approach, the largest $\Delta\tau$ for a stable solution is somewhere near 0.1. As shown in Fig. 1, the solution with the fully implicit

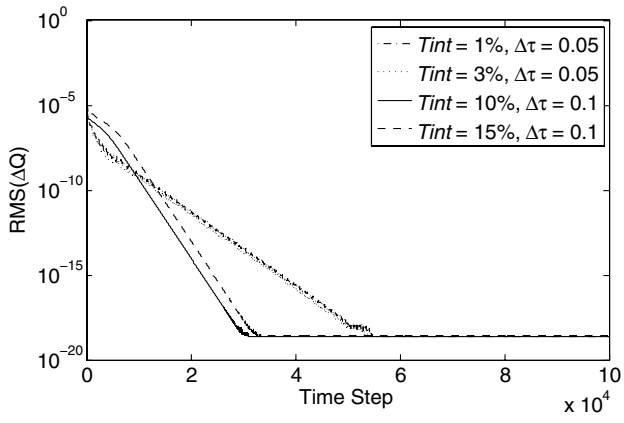

a) $k - \varepsilon$ solution vector residual vs time step

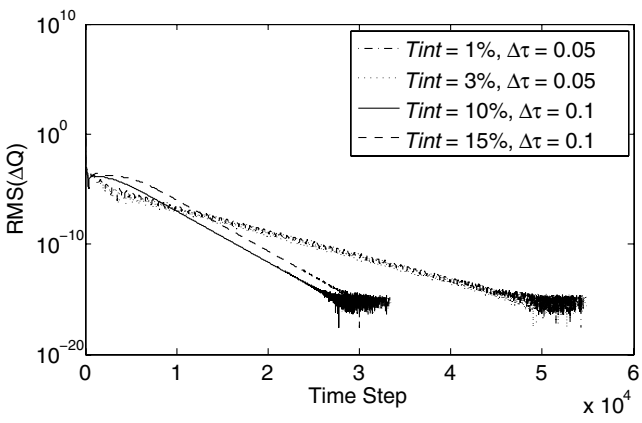

b) Mean flow solution vector residual vs time step

Fig. 2 Convergence history for fully developed flow, $Re = 7700$: change in the root mean square residual, RMS-DELQ, of the solution vector between two successive time levels.

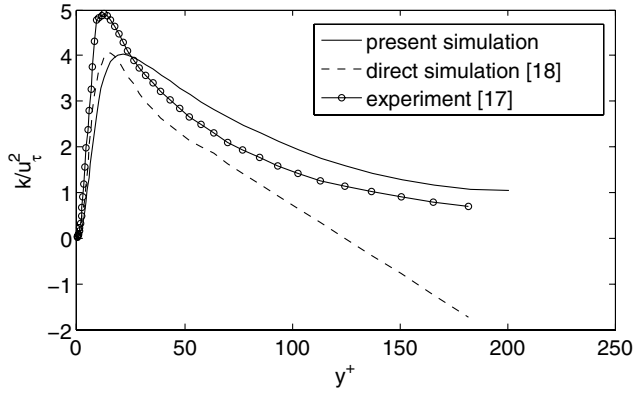

a) k/u_τ^2 vs the wall coordinate

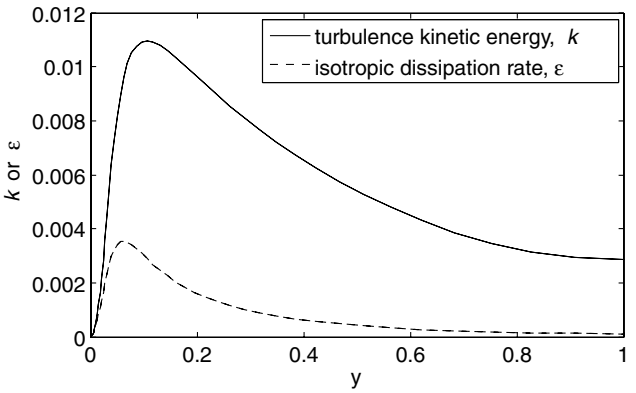

b) k and ε along the channel height

Fig. 3 Variation of turbulence kinetic energy, k, and isotropic dissipation rate, ϵ, along the channel height; fully developed flow; $Re = 7700$.

technique converges to machine accuracy within about 30,000 time steps, and with the semi-implicit technique, its convergence to machine accuracy is achieved within about 550,000 time steps illustrating a convergence speed up of about 2 orders of magnitude As a note, a convergence speed up of well over 3 orders of magnitude was observed for the case of downstream developing turbulence in the channel, as shown in the next section. This has to do with the interaction between the particular mean flow solution technique used and the present transport equation solution technique for the downstream developing turbulence. However, the conclusions on the convergence characteristics of the transport equation solution methodology presented here are best discussed without the extraneous influence of the mean flow solution methodology.

Three more fully developed simulations at $Re = 7700$ were carried out with three different initial conditions corresponding to three turbulence intensities, $T_{\text{int}} = 0.01$, 0.03, and 0.15. It should be noted here that for the case of $T_{\text{int}} = 0.01$ and 0.03, time step $\Delta\tau$ had to be decreased from 0.1 to 0.05 for a stable solution, although for $T_{\text{int}} = 0.1$ and 0.15, $\Delta\tau = 0.1$ yielded a stable solution. This is due to the reason that the lower the turbulence intensity, the more stiff the k-ϵ system becomes. Figure 2a shows some differences in the convergence histories. The main difference is due to the size of the time step used for different initial conditions. The initial conditions corresponding to the lower turbulence intensities, $T_{\text{int}} = 0.01$ and 0.03 yield a converged solution after about 55,000 time steps, and for $T_{\text{int}} = 0.1$ and 0.15, solutions converge after about 30,000 time steps. Corresponding results for the mean flow solution convergence are shown in Fig. 2b. Similar convergence behavior is exhibited by the mean flow solution.

A converged near-wall variation of turbulence kinetic energy with the wall variable, y^+, corresponding to $Re = 7700$, is shown in Fig. 3a. A comparison of the present predictions with the experiment [17] and the direct numerical simulation [18] shows a reasonable agreement with the experiment away from the wall and with the direct simulation closer to the wall. Variation of k and the isotropic dissipation rate ϵ along the channel height is shown in Fig. 3b. The extent to which the present simulation agrees with the experiment [17] is as expected, since the accuracy of the predictions has to do with the particular k-ϵ model [3] used and not the numerical method used here.

Another fully developed simulation at $Re = 12,300$ was carried out and the corresponding results are compared with the well-known Pai profile [19] calibrated for $Re = 12,300$. Comparison with the well-established Pai profile shows excellent agreement between the present simulation and the Pai profile for the Reynolds stress normal to the wall in Fig. 4, except that the peak values of the Pai profile are somewhat underpredicted. Figure 4 shows a similar comparison of fully developed turbulent velocity profile between the present simulation and the Pai profile that is shown to be very good.

B. Developing Flow Simulations

Following discussion relates to the case of downstream developing flow in the channel at $Re = 12,300$. Three simulations were carried out for this purpose. These simulations were carried out for a developing turbulent channel flow, with the specific purpose of assessing the influence of the inflow k and ϵ conditions on the turbulent flow evolving downstream. For this case, a fully viscous artificial compressibility solver [20] with temperature equation, a variant of INS3D solver [21], was used. The artificial compressibility formulation proposed by Chorin [22] was used to solve the internal flow equations in generalized curvilinear coordinates. In the present simulations, the artificial compressibility parameter, β, was found to have a dependence on T_{int}, as observed below. For further analysis on the choice of β, the reader is referred to Kwak and Chang [23]. Second-order extrapolation on pressure and the velocity components

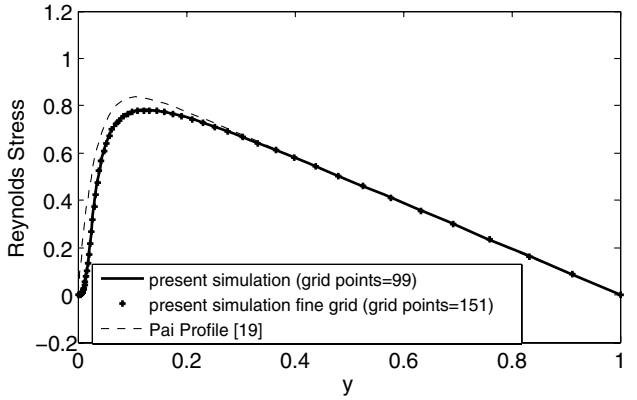

a) Reynolds stress, $-\overline{u'v'}/u_\tau^2$, variation

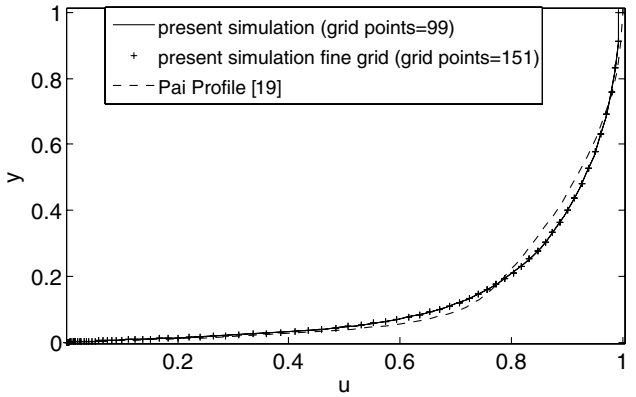

b) Streamwise velocity variation

Fig. 4 Variation along the channel height; fully developed flow; $Re = 12,300$.

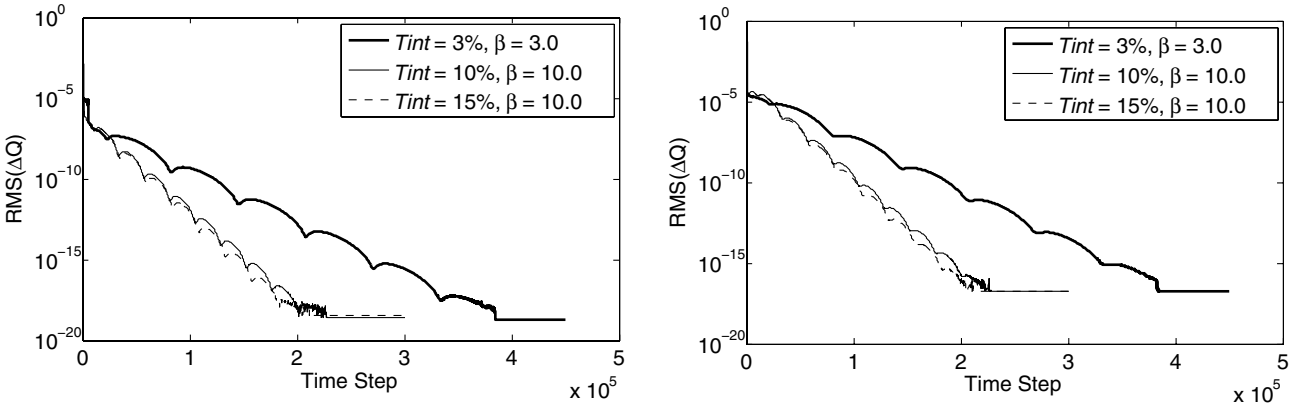

a) $k-\varepsilon$ solution vector residual vs time step

b) Mean flow solution vector residual vs time, τ

Fig. 5 Convergence history for developing flow, $Re = 12,300$, with the fully implicit method: change in the rms residual, RMS-DELQ, of the solution vector between two successive time levels.

was used at the outflow boundary. Fixed mass flux through the channel was enforced by scaling the outlet velocity appropriately. Three different levels of turbulence intensity, $T_{\text{int}} = 3$, 10 and 15%, were chosen to demonstrate the effect of inflow boundary conditions.

A 99×99 grid, uniformly stretched in the streamwise direction, was used for the developing flow simulations. With a uniform flow entering the channel at the inlet, it is well known that it takes turbulent flow hundreds of channel heights to attain a fully developed profile downstream. An appropriate grid used for this simulation was chosen to be 500 channel heights long, as suggested by Rotta's pipe flow experiments [24] where at a Reynolds number of 2500, the flow takes 500 pipe diameters downstream to attain an intermittency factor of about 85%. In our case, since the channel Reynolds number is 12,300 and the inflow is turbulent, it is reasonable to expect that the turbulent flow will have become fully developed at 500 channel heights downstream. As we shall see numerically, the flow does attain a fully developed state at the channel outlet.

It should be noted here that for all the three cases, a time step size of 0.08 yields a stable solution. A value of $\beta = 3.0$ was used for $T_{\text{int}} = 0.03$, and for $T_{\text{int}} = 0.1$ and 0.15, $\beta = 10.0$ was used. As T_{int} decreases, the stable value of β also decreases. This is due to the fact that at lower turbulence intensity levels, the k-ϵ system becomes very stiff and hence requires a slower rate of relaxation to steady-state through the artificial compressibility formulation. There is also a dependence of β on $\Delta\tau$ [23] that serves as an additional guide for the proper choice of β. Convergence results are shown in Figs. 5a and 5b.

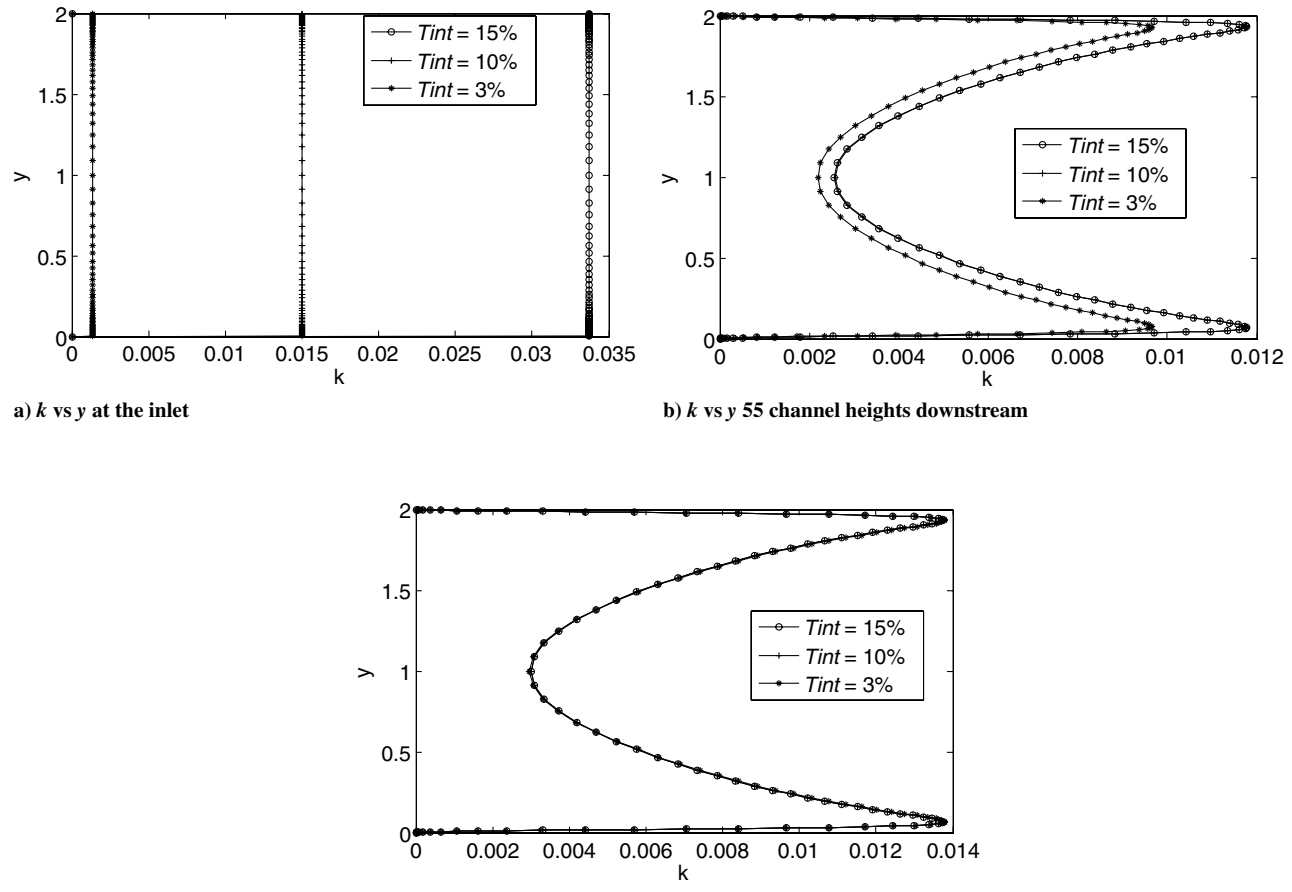

a) k vs y at the inlet

b) k vs y 55 channel heights downstream

c) k vs y at the outlet

Fig. 6 Developing flow: turbulence kinetic energy k profiles at three streamwise stations corresponding to three different inlet turbulence levels; $Re = 12,300$.

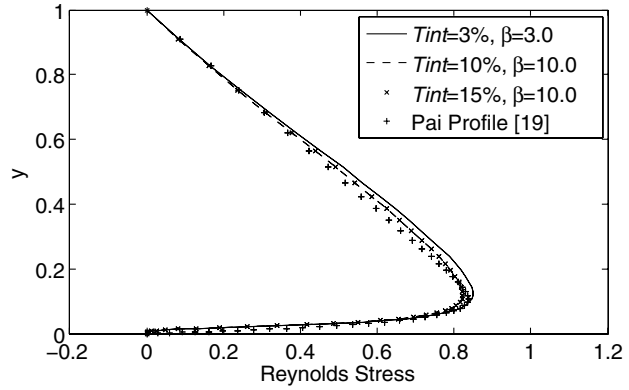

Fig. 7 Developing flow: Reynolds stress at the channel outlet, $-\overline{u'v'}/u_\tau^2$, profiles corresponding to three different inlet turbulence levels; $Re = 12,300$.

Figures 5a and 5b show that the k-ϵ and the mean flow solutions converge to machine accuracy at nearly the same time: 230,000 steps for higher inlet turbulence intensity levels, and 380,000 time steps for the 3% inlet turbulence intensity level.

Figures 6a–6c show the turbulence kinetic energy profiles at the inlet, at a downstream location and at the outlet, corresponding to the three levels of inlet turbulence intensity. Figure 6a shows the inflow boundary prescription of k at the three turbulence intensity levels. The flow has attained a fully developed state at the outlet, and hence the k profiles shown in Fig. 6c corresponding to the three different inflow boundary conditions are practically identical. But, at a station between the inlet and the outlet, about 55 channel heights downstream, the k profiles, as shown in Fig. 6b, differ measurably. This delineates the need for a thoughtful prescription of inflow boundary conditions on k in internal flows. A comparison is shown for Reynolds stress, $-\overline{u'v'}/u_\tau^2$, at the outlet corresponding to the three inlet boundary conditions in Fig. 7, confirming that the flow at the outlet has almost attained the fully developed state. Whereas there is some discrepancy between the Pai profile [19] and the simulation corresponding to $T_{i\text{int}} = 0.03$, the simulations with the other two turbulence intensity levels, $T_{\text{int}} = 0.10$ and 0.15, are in better agreement with the Pai profile. This demonstrates that higher levels of turbulence intensity at the channel inlet result in a faster relaxation to the fully developed state downstream and hence better agreement with the Pai profile.

Finally, two revealing simulations of developing flow with two different time steps are made with the semi-implicit method and $T_{\text{int}} = 0.15$ at the inlet. Convergence histories of the mean flow solution with $\Delta\tau$= 8E-05 and $\Delta\tau$= 1E-05 are contrasted in Fig. 8. It is shown that for $\Delta\tau$= 8E-05, even though it is 3 orders of magnitude smaller than $\Delta\tau$ used for a converged solution with the fully implicit method (Fig. 5), the semi-implicit solution still diverges at about 100,000 time steps. On further decreasing $\Delta\tau$ to 1E-05, the semi-implicit solution begins to limp along stably, but its convergence rate is very low. At about 900,000 time steps, it has converged only to accuracy of about 1.E-05. Thus it is clear that the present fully implicit method is more than 3 orders of magnitude faster in convergence than the semi-implicit method. Corresponding convergence history for the k-ϵ turbulence solution is also shown in Fig. 8 for added comparison.

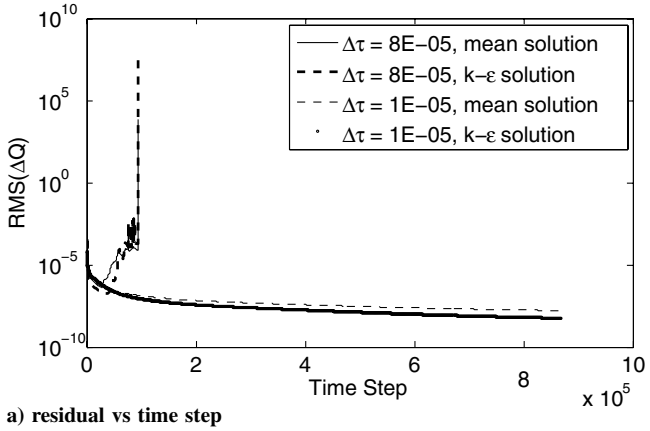

a) residual vs time step

Fig. 8 Convergence history for developing flow, $Re = 12,300$, with the semi-implicit method: change in the root mean square residual, RMS-DELQ, of the solution vectors between two successive time levels.

V. Conclusions

A fully implicit approximate factorization technique for the solution of transport equations in fluid dynamics based on the ΔQ algorithm of Beam–Warming and Briley–McDonald has been presented here. The fully implicit technique has reliably demonstrated the effect of inflow turbulent kinetic energy and the dissipation rate boundary conditions on the downstream developing flow in a channel. While the effect of initial conditions on a fully developed flow is not significant, the effects of inflow boundary conditions for a developing flow are clearly substantial. For the fully developed flow, the implicit technique results in 2 orders of magnitude improvement in convergence to steady state over the semi-implicit method [5,7]. Quite remarkably, for a downstream developing flow, convergence with the fully implicit method is about 4 orders of magnitude faster as compared with the semi-implicit method. The present fully implicit method is general and can be applied to the solution of any transport equation system. Driving the solution convergence to machine accuracy is an essential requirement to reliably assess the effects of inflow boundary conditions on the downstream developing flow.

Acknowledgments

This work was funded by the Supersonics Project of the NASA Fundamental Aeronautics Program during the development of a compressible Reynolds Averaged Navier–Stokes solver, EDLFLOW (mean flow) and SUPKEM (k-ϵ turbulence solver). Results from EDLFLOW will be reported later. The author would like to acknowledge helpful comments during the review process.

References

[1] Jones, W. P., and Launder, B. E., "Prediction of Low Reynolds Number Phenomena with a Two-Equation Model of Turbulence," *International Journal of Heat and Mass Transfer*, Vol. 16, No. 6, June 1973, pp. 1119–1130. doi:10.1016/0017-9310(73)90125-7

[2] Kaul, U. K., and Frost, W., "Turbulence Atmospheric Flow Over a Backward-Facing Step," NASA CR-2749, Oct. 1976.

[3] Chien, K. Y., "Predictions of Channel and Boundary-Layer Flows with a Low-Reynolds-Number Turbulence Model," *AIAA Journal*, Vol. 20, January 1982, pp. 33–38. doi:10.2514/3.51043

[4] Kaul, U. K., and Kwak, D., "Computation of Internal Turbulent Flow With a Large Separated Flow Region," *International Journal for Numerical Methods in Fluids*, Vol. 6, No. 12, 1986, pp. 927–937. doi:10.1002/fld.1650061206

[5] Kaul, U. K., "An Implicit Finite-Difference Code for a Two-Equation Turbulence Model for Three-Dimensional Flows," NASA TM-86752, June 1985.

[6] Sahu, J., and Danberg, J. E., "Navier-Stokes Computations of Transonic Flows with a Two-Equation Turbulence Model," *AIAA Journal*, Vol. 24, No. 11, Nov. 1986, pp. 1744–1751.

[7] Kaul, U. K., "Turbulent Flow in a 180° Bend: Modeling and Computations," NASA CR-4141, June 1988.

[8] Kandula, M., and Pearce, D. G., "Three-Dimensional Navier–Stokes Simulation of Space-Shuttle Main Propulsion 17-inch Disconnect Valves," *Journal of Propulsion and Power*, Vol. 7, No. 3, 1991, pp. 330–340. doi:10.2514/3.23331

[9] Williams, M., "The Solution of the 2-Dimensional Incompressible-Flow Equations on Unstructured Triangular Meshes," *Numerical Heat Transfer*, Vol. 23, No. 3, 1993, pp. 309–325. doi:10.1080/10407799308914903

[10] Kaul, U. K., "A Fully Implicit Numerical Scheme for the Solution of Transport Equations in Fluid Dynamics," *International Conference on Numerical Methods in Laminar and Turbulent Flow*, Stanford Univ., Palo Alto, CA,1991.

[11] Beam, R. M., and Warming, R. F., "An Implicit Factored Scheme for Compressible Navier–Stokes Equations," *AIAA Journal*, Vol. 16, No. 4, 1978, pp. 393–402.

[12] Briley, W. R., and McDonald, H., "Solution of the Three-Dimensional Compressible Navier–Stokes Equations by an Implicit Technique," *Proceedings of the 4th International Conference on Numerical Methods in Fluid Dynamics*, Lecture Notes in Physics, Vol. 35, Springer–Verlag, New York, 1975, pp. 105–110.

[13] Sarkar, S., Erlebacher, G., Hussaini, M. Y., and Kreiss, H. O., "The Analysis and Modeling of Dilatational Terms in Compressible Turbulence," *Journal of Fluid Mechanics*, Vol. 227, June 1991, pp. 473–495.
doi:10.1017/S0022112091000204

[14] Abdol-Hamid, K. S., Frink, N. T., Deere, K. A., and Pandya, M. J., "Propulsion Simulations Using Advanced Turbulence Models with the Unstructured Grid CFD Tool, TetrUSS," AlAA Paper 2004-0714, Jan. 2004.

[15] Hanjalic, K., and Launder, B. E., "Contribution Towards a Reynolds-Stress Closure for Low-Reynolds-Number Turbulence," *Journal of Fluid Mechanics*, Vol. 74, No. 4, April 1976, pp. 593–610.
doi:10.1017/S0022112076001961

[16] Taylor, G. I., "The Transport of Vorticity and Heat Through Fluids in Turbulent Motion," *Philosophical Transactions of the Royal Society of London, Series A: Mathematical and Physical Sciences*, Vol. 215, No. I-26, 1915.

[17] Kreplin, H-P., and Eckelmann, H., "Behavior of the Three Fluctuating Velocity Components in the Wall Region of a Turbulent Channel Flow," *Physics of Fluids*, Vol. 22, No. 7, 1979, pp. 1233–1239.
doi:10.1063/1.862737

[18] Kim, J., Moin, P., and Moser, R., "Turbulence Statistics in Fully Developed Channel Flow at Low Reynolds Number," *Journal of Fluid Mechanics*, Vol. 177, 1987, pp. 133–166.
doi:10.1017/S0022112087000892

[19] Pai, S. I., "On Turbulent Flow Between Parallel Plates," *Journal of Applied Mechanics*, Vol. 20, No. 1, 1953, pp. 109–114.

[20] Kaul, U. K., and Shreeve, R. P., "Full Viscous Modeling in Generalized Coordinates of Heat Conducting Flows in Rotating Systems," *Journal of Thermophysics and Heat Transfer*, Vol. 10, No. 4, Oct.–Dec. 1996, pp. 621–626.
doi:10.2514/3.838

[21] Kwak, D., Chang, J. L. C., Shanks, S. P., and Chakravarthy, S. R., "A Three-Dimensional Incompressible Navier-Stokes Flow Solver Using Primitive Variables," *AIAA Journal*, Vol. 24, No. 3, 1986, pp. 390–396.
doi:10.2514/3.9279

[22] Chorin, A. J., "A Numerical Method for Solving Incompressible Viscous Flow Problems," *Journal of Computational Physics*, Vol. 2, No. 1, 1967, pp. 12–26.
doi:10.1016/0021-9991(67)90037-X

[23] Kwak, D., and Chang, J. L. C., "On the Method of Pseudo-Compressibility for Numerically Solving Incompressible Flows," AIAA Paper 84-0252, 1984.

[24] Rotta, J., "Experimental Contributions to the Development of Turbulent Flow in a Pipe," *Archives of Engineering*, Vol. 24, 1956, pp. 258–281.

J. Sahu
Associate Editor